# $Ba_6Ti_5S_{15}O$: A New Metal/Oxysulfide Resulting from the Inclusion of BaO into the $BaTiS_3$ Structure Type

Anthony C. Sutorik and Mercouri G. Kanatzidis*,†

*Department of Chemistry and Center for Fundamental Materials Research, Michigan State University, E. Lansing, Michigan 48824*

*Received March 11, 1994. Revised Manuscript Received June 3, 1994*®

From a mixture of 0.212 g BaS (1.25 mmol), 0.038 g BaO (0.25 mmol), 0.060 g Ti (1.25 mmol), and 0.080 g S (2.50 mmol) heated in a quartz tube at 700 °C for 8 days, we have synthesized $Ba_6Ti_5S_{15}O$. The compound crystallizes in the $C222_1$ space group (No. 20) with $a$ = 6.708(5) Å, $b$ = 15.683(4) Å, $c$ = 23.740(7) Å, and $V$ = 2497(2) Å$^3$ final ($R/R_w$ = 3.8%/5.4%). The structure is two-dimensional and features $[Ti_5S_{15}O]$ fragments composed of five face-sharing Ti centered octahedra with O atoms occupying one site on each terminal face. These fragments are then joined together through linear bridges at the O atom and one S atom of the terminal face into the 2D layer. The $Ba^{2+}$ cations reside in intralayer cavities, leaving the space between the layers open. Diffuse reflectance measurements show an absorption edge at approximately 1.04 eV, indicating semiconducting behavior.

## Introduction

In solid-state chemistry, a classic synthetic approach to new materials is to modify a known structure type by forcing it, usually through reactions at very high temperatures, to adapt to the inclusion of elements (compositional or structural) from other compounds. This approach can result in new materials possessing recognizable structural fragments of one or both of the starting compounds. In some cases this has led to whole families of related phases in which the size or quantity of the known structural fragments are varied depending on the amount of the second compound "forced in". One such well-known system is $(ZnS)_n(In_2S_3)_m$,[1] and several other examples of new alkali metal/transition metal/chalcogenides have been synthesized in our lab from reactions in molten alkali metal polychalcogenides ($A_2Q_x$) at intermediate temperatures (250-450 °C).[2] We had been curious as to whether the methodologies of the $A_2Q_x$ fluxes could be extended to alkaline-earth polychalcogenides as well. It was during investigation of Ti reactivity in molten $BaS_x$ fluxes that we first observed the new oxysulfide $Ba_6Ti_5S_{15}O$. Subsequently prepared from a stoichiometric combination of BaS/BaO/Ti/S, this compound represents the first member of a potential new family of materials with the general formula $(BaO)_n(BaTiS_3)_m$. As implied by this formalism, $Ba_6Ti_5S_{15}O$ is structurally related to $BaTiS_3$ in that the infinite chains of $[TiS_6]$ face-sharing octahedra of the ternary compound have been fragmented and reconnected into a two-dimensional layered structure by inclusion of BaO.

The discovery of $Ba_6Ti_5S_{15}O$ is also notable in that solid state oxychalcogenide compounds (i.e., compounds in which $S^{2-}$ and $O^{2-}$ are discrete rather than combined in an anionic unit) are generally rare. Known examples are dominated by lanthanide containing species, in both ternary[3] and quaternary systems.[4] For transition metals ZrOS and HfOS are the only known ternary compounds[5] with extended structures, but a compound composed of discrete anionic clusters is found in $Ba_6(NbS_4)(NbS_3O)$.[6] Several quaternary phases containing transition metals exist, but they also possess a lanthanide as one of the components. These consist of the layered phases $Fe_2La_2O_3Q_2$ (Q = S, Se)[7] and MLaOS (M = Cu, Ag)[4] and the three-dimensional structures of $CrLnOS_2$,[8] $CrLaOSe_2$,[8] $V_3La_5O_7S_6$,[9] $La_2Ta_3O_8S_2$,[10a] and $Ln_2Ta_3O_8Se_2$ [10b] (Ln = lanthanide). Oxy-chalcogenide compounds of the main-group elements include the mineral kesmesite, $Sb_2S_2O$,[11] and $Bi_2O_2Q$ (Q = S, Se).[12] The general investigation into oxychalcogenides has no doubt been inhibited by the high stability of the polyatomic anions and binary metal oxides, both of which

† A. P. Sloan Foundation Fellow 1991-93 and Camille and Henry Dreyfus Teacher Scholar 1993-95.

® Abstract published in *Advance ACS Abstracts,* July 1, 1994.

(1) (a) Donika, F. G.; Klosse, G. A.; Radautsan, S. I.; Semiletov, S. A.; Zhitar, V. F. *Sov. Phys.-Crystallogr. (Engl. Transl.)* **1968**, *12*, 745-749. (b) Boorman, R. S.; Sutherland, J. K. *J. Mater. Sci.* **1969**, *4(8)*, 658-671. (c) Barnett, D. E.; Boorman, R. S.; Sutherland, J. K. *Phys. Status Solidi A* **1971**, *4(1)*, K49-K52.

(2) Kanatzidis, M. G. *Chem. Mater.* **1990**, *2*, 353-363.

(3) The three phases most commonly encountered are $Ln_2O_2Q$, $Ln_2O_2(S_2)$ and $Ln_4O_4S(Se_2)$, Ln = lanthanide and Q = chalcogenide. Flauhaut, J. In *Handbook on the Physics and Chemistry of Rare Earths;* Gschneidner, Jr., K. A., Eyring, L., Ed.; North-Holland: Amsterdam, 1979; Vol. 4. p 1-88.

(4) Guittard, M.; Benazeth, S.; Dugué, J.; Jaulmes, S.; Palazzi, M.; Laruelle, P.; Flauhaut, J. *J. Solid State Chem.* **1984**, *51*, 227-238.

(5) (a) Wells, F. A. *Structural Inorganic Chemistry,* 5th ed. Carendon: Oxford, 1984; pp 786-787. (b) Eisman, G. A.; Steinfink, H. *J. Solid State Chem.* **1982**, *43*, 225-226. (c) Eisman, G. A.; Swinnea, J. S.; Steinfink, H. *J. Solid State Chem.* **1985**, *56*, 397-398.

(6) Rendon-Diazmiron, L. E.; Campana, C. F.; Steinfink, H. *J. Solid State Chem.* **1983**, 47, 322-327.

(7) Mayer, J. M.; Schneemeyer, L. F.; Siegrist, T.; Waszczak, J. V.; Van Dover, B. *Angew. Chem., Int. Ed. Engl.* **1992**, *31*, 1645-1647.

(8) (a) Vovan, T.; Dugué, J.; Guittard, M. *Mater. Res. Bull.* **1978**, *13*, 1163-1166. (b) Dugué, J.; Vovan, T., Viller, J. *Acta Crystallogr. Sect. B* **1980**, *36*, 1291-1294. (c) Winterberger, M.; Vovan, T.; Guittard, M. *Solid State Commun.* **1985**, *53*, 227-230. (d) Winterberger, M.; Dugué, J.; Guittard, M.; Dung, N. H.; Vovan, T. *J. Solid State Chem.* **1987**, *70*, 295-302.

(9) Dugué, J., Vovan, Laruelle, P. *Acta Crystallogr. Sect. C* **1985**, *41*, 1146-1148.

(10) (a) Brennan, T. D.; Aleandri, L. E.; Ibers, J. A. *J. Solid State Chem.* **1991**, *91*, 312-322. (b) Brennan, T. D.; Ibers, J. A. *J. Solid State Chem.* **1992**, *98*, 82-89.

(11) Baumgardt, E. M.; Kupcik, V. *J. Cryst. Crowth* **1977**, *37*, 346.

(12) (a) Koyama, E.; Nakai, I.; Nagashima, K. *Acta Crystallogr.* **1984**, *B40*, 105-109. (b) Boller, H. *Monatsch. Chem.* **1973**, *104*, 916-919.

0897-4756/94/2806-1700$04.50/0 

would be the most likely thermodynamic roadblocks to new compound formation. Given this lack of exploration, it is likely that the synthesis of $Ba_6Ti_5S_{15}O$ could provide some relevant lessons in the search for new oxychalcogenide materials.

## Experimental Section

The following materials were used as obtained: BaS, 100 mesh, 99.999% purity, Cerac, Milwaukee, WI; BaO, 100 mesh, 99.5% purity, Cerac, Milwaukee, WI; Ti metal, 325 mesh, Alfa, Danvers, MA; and sulfur powder, sublimed, JT Baker Co., Phillipsburg, NJ.

As mentioned in the introduction, $Ba_6Ti_5S_{15}O$ was first isolated from the reaction of Ti metal in excess $BaS_x$. BaS (0.271 g, 1.6 mmol), Ti (0.019 g, 0.4 mmol), and S (0.102 g, 3.2 mmol) were mixed in a nitrogen-filled glovebox and loaded into quartz tubes, which were subsequently evacuated on a Schlenk line to $<3 \times 10^{-3}$ mbar and flame-sealed. The reagents were heated in a computer-controlled furnace to 600 °C over 6 h and left at that temperature for 6 days, followed by cooling at 4 °C/h to 440 °C and quenching to 50 °C. The excess $BaS_x$ flux was removed by dissolving it with degassed distilled water under $N_2$ flow. Washings were continued until the solvent no longer turned yellow, signaling that all the polysulfide had been removed. The sample was then dried under vacuum. The major phase from this preparation was very small blue needles of $BaTiS_3$. $Ba_6Ti_5S_{15}O$ was present as a very minor phase but grew as large gray plates which could be manually extracted from the bulk of the product. Single-crystal diffraction studies were performed on samples synthesized from the above reaction. The large plates are insoluble in methanol and dimethylformamide, as well as water, and appear stable in air for extended periods.

The original source of oxygen was determined to be contamination from an aged supply of BaS as switching to a freshly obtained batch yielded only the ternary compound. Initial attempts at rational reproduction of the oxysulfide were made using fresh BaS and BaO, which was added in a 1/5 ratio to the Ti metal in the above reaction. This approach saw no increase in the yield of $Ba_6Ti_5S_{15}O$, which still occurred as large plates in very small yield. The major phase was still $BaTiS_3$ but was now accompanied by a significant amount of $TiO_2$, as determined by powder X-ray diffraction. The added diffusion which the excess $BaS_x$ provides, although excellent for crystal growth, apparently allowed for too much oxide mobility and hence led to a portion of the very oxophilic $Ti^{4+}$ being converted to $TiO_2$.

Pure $Ba_6Ti_5S_{15}O$ was successfully synthesized at high temperature from a reaction of BaS/BaO/Ti/S in the exact stoichiometric ratio of the compound: 0.212 g BaS (1.25 mmol), 0.038 g BaO (0.25 mmol), 0.060 g Ti (1.25 mmol), and 0.080 g S (2.5 mmol). The reagents were mixed and loaded into quartz tubes as described above. The tubes were evacuated to $<2 \times 10^{-4}$ mbar and flame sealed. Samples were heated to 700 °C in 12 h and isothermed at that temperature for 8 days followed by cooling to 500 °C at 4 °C/h and quenching to 50 °C. A small amount of residual $BaS_x$ still remained, and so the product was washed with degassed distilled water as described earlier. The remaining material was a gray microcrystalline powder. EDS analysis reveals Ba, Ti, and S in an approximate 1/1/3 ratio. Oxygen cannot be detected by this technique because its emission lines lie below the lower detection limit of the system. The powder X-ray diffraction pattern of the product corresponded to that calculated for $Ba_6Ti_5S_{15}O$ from single-crystal diffraction data (Table 1); no other peaks from $BaTiS_3$, $TiO_2$, or any other impurity were detected. As control experiments, this procedure was also performed with several modifications. First, omission of BaO from the reaction resulted in only $BaTiS_3$ as the final product. Second, by shortening the isotherm time to 2 days, $BaTiS_3$ was again found to be the major phase, implying that the oxysulfide is a thermodynamic product, forming after BaO has a chance to act upon the ternary. Also since most of the flux is consumed in the initial formation of the ternary, the diffusion of oxide through the sample is increasingly limited as the reaction progresses. As such $TiO_2$, one of the byproducts of the reaction, is avoided while the high oxophilicity of $Ti^{4+}$ is still strong enough to drive the formation of the quaternary despite the limited diffusion.

**Table 1. Calculated and Observed X-ray Powder Diffraction Patterns for $Ba_6Ti_5S_{15}O$ (Cu Radiation)**

| $h\,k\,l$ | $d_{calc}$ | $d_{obs}$ | $\%\ I/I_{0\ obs}$ |
|---|---|---|---|
| 0 2 1 | 7.44 | 7.51 | 5.52 |
| 0 2 2 | 6.54 | 6.60 | 2.38 |
| 1 1 2 | 5.47 | 5.51 | 2.16 |
| 1 1 3 | 4.86 | 4.894 | 3.42 |
| 1 1 4 | 4.24 | 4.298 | 24.41 |
| 1 3 1 | 4.06 | 4.085 | 7.22 |
| 0 0 6 | 3.957 | 3.978 | 80.20 |
| 0 4 0 | 3.921 | 3.938 | 92.22 |
| 0 4 1 | 3.868 | 3.781 | 11.17 |
| 1 3 3 | 3.657 | 3.676 | 8.85 |
| 2 0 0 | 3.386 | 3.401 | 46.31 |
| 1 3 4 | 3.354 | 3.368 | 38.16 |
| 2 0 1 | 3.321 | 3.339 | 9.04 |
| 1 3 5 | 3.113 | 3.126 | 15.88 |
| 2 2 0 | 3.092 | 3.095 | 3.45 |
| 2 2 2 | 2.985 | 2.995 | 6.81 |
| 0 4 6 | 2.785 | 2.794 | 100.00 |
| 1 5 2, 2 0 5 | 2.737 | 2.748 | 15.19 |
| 0 2 8 | 2.674 | 2.687 | 9.16 |
| 1 3 7 | 2.619 | 2.622 | 26.23 |
| 2 0 6 | 2.559 | 2.561 | 71.58 |
| 1 5 4 | 2.549 | 2.543 | 9.98 |
| 0 6 2 | 2.500 | 2.509 | 11.01 |
| 1 5 5 | 2.438 | 2.445 | 3.26 |
| 1 5 5, 1 3 8 | 2.409 | 2.417 | 6.96 |
| 1 3 8, 0 6 4 | 2.392 | 2.389 | 7.37 |
| 2 0 7 | 2.385 | 2.380 | 7.72 |
| 2 0 8 | 2.222 | 2.225 | 7.94 |
| 2 4 6 | 2.143 | 2.146 | 5.11 |
| 1 7 2 | 2.092 | 2.097 | 5.14 |
| 1 3 10 | 2.057 | 2.060 | 7.66 |
| 2 6 2 | 2.030 | 2.036 | 7.97 |
| 2 2 9 | 2.008 | 2.006 | 13.99 |
| 0 0 12 | 1.978 | 1.985 | 3.73 |
| 0 8 0 | 1.960 | 1.967 | 24.32 |
| 3 3 5 | 1.888 | 1.890 | 4.02 |
| 0 6 9 | 1.856 | 1.861 | 3.07 |
| 0 4 12 | 1.766 | 1.768 | 6.12 |
| 2 6 8 | 1.683 | 1.697 | 7.03 |
| 4 0 1 | 1.673 | 1.678 | 4.42 |
| 3 7 2 | 1.568 | 1.564 | 4.17 |

**Physical Measurements.** *Powder X-ray Diffraction.* Analyses were performed using a calibrated Rigaku Rotaflex rotating anode powder diffractometer controlled by an IBM computer and operating at 45 kV/100 mA, employing Ni-filtered Cu radiation.

*Infrared Spectroscopy.* Infrared spectra, in the far-IR region (600–50 $cm^{-1}$), were recorded on a computer-controlled Nicolet-740 Fourier transform infrared spectrophotometer in 4 $cm^{-1}$ resolution. Analyses were performed on solid samples using CsI as the pressed pellet matrix.

*UV/Vis/Near IR Spectroscopy.* Optical diffuse reflectance measurements were performed at room temperature using a Shimadzu UV-3101PC double-beam, double-monochromator spectrophotometer. The instrument is equipped with integrating sphere and controlled by personal computer. The reflectance versus wavelength data generated can be used to estimate the band gap by converting reflectance to absorption data using the Kubelka–Munk function as described elsewhere.[13]

*Single Crystal X-ray Diffraction.* Intensity data for $Ba_6Ti_5S_{15}O$ was collected at 23 °C with Mo Kα radiation using a Rigaku AFC6S four-circle automated diffractometer equipped with a graphite crystal monochromator. The $\omega-2\theta$ scan mode was used. The crystal stability was monitored with three

(13) McCarthy, T. J.; Ngeyi, S.-P.; Liao, J.-H.; DeGroot, D. C.; Hogun, T.; Kannewurf, C. R.; Kanatzidis, M. G. *Chem. Mater.* **1993**, *5*, 331–340.

**Table 2. Fractional Atomic Coordinates and $B_{eq}$[a] Values for $Ba_6Ti_5S_{15}O$ with Estimated Standard Deviations in Parentheses**

| atom | $x$ | $y$ | $z$ | $B_{eq}$ |
|---|---|---|---|---|
| Ba(1) | 0.2074(2) | 0.89125(5) | 0.33673(4) | 1.31(3) |
| Ba(2) | 0.7029(2) | 0.85576(6) | 0.48386(4) | 1.39(3) |
| Ba(3) | 0.2810(1) | 0.90019(5) | 0.82219(3) | 0.99(3) |
| Ti(1) | −0.1944(5) | 1.2580(2) | 0.1946(1) | 1.1(1) |
| Ti(2) | 0.2315(4) | 1.1286(2) | 0.4053(1) | 1.12(9) |
| Ti(3) | 0.1855(6) | 1 | 1/2 | 1.3(1) |
| S(1) | 0 | 0.7451(4) | 1/4 | 1.4(2) |
| S(2) | −0.2095(8) | 1.4014(2) | 0.1950(2) | 1.6(1) |
| S(3) | 0.2146(7) | 1.0880(2) | 0.3087(1) | 1.0(1) |
| S(4) | 0.4538(6) | 1.2368(3) | 0.3907(2) | 1.1(1) |
| S(5) | −0.0272(6) | 1.2386(3) | 0.3855(2) | 1.0(1) |
| S(6) | −0.0469(6) | 0.9828(3) | 0.5738(2) | 1.1(1) |
| S(7) | −0.5460(6) | 1.0148(3) | 0.4273(2) | 1.0(1) |
| S(8) | 0.7956(7) | 0.8467(2) | 0.4924(1) | 1.0(1) |
| O | 1/2 | 0.743(1) | 1/4 | 1.7(7) |

[a] $B$ values for anisotropically refined atoms are given in the form of the isotropic equivalent displacement parameters defined as $B_{eq} = {}^4/_3a^2B(1,1) + b^2B(2,2) + c^2B(3,3) + ab(\cos\gamma)B(1,2) + ac(\cos\beta)B(1,3) + bc(\cos\alpha)B(2,3)$.

standard reflections whose intensities were checked every 150 reflections. No decay was detected. The range of *hkl* reflections collected was from 000 to *hkl* (an octant of a reciprocal lattice sphere). An empirical absorption correction based on $\psi$ scans was applied to all data during initial stages of refinement. The range of transmission factors was 0.134 to 0.99 with an average of 0.652. No extincion correction was employed. An empirical DIFABS correction[14] was applied after full isotropic refinement, followed by full anisotropic refinement. The structure was solved by direct methods using SHELXS-86 software,[15a] and full-matrix least-squares refinement was performed using the TEXSAN software package.[15b] Atomic scattering factors were obtained from ref 15b.

Crystals of $Ba_6Ti_5S_{15}O$ (size 0.1 × 0.4 × 0.5 mm$^3$) were determined to be of the orthorhombic space group $C222_1$ (No. 20) with $a$ = 6.708(5) Å, $b$ = 15.683(4) Å, $c$ = 23.740(7) Å, $V$ = 2497(2) Å$^3$, $Z$ = 4, $D_{calc}$ = 4.15 g/cm$^3$, $\mu$ = 123 cm$^{-1}$, $2\theta_{max}$ = 60.00. The total number of data collected was 2069, with 2052 being unique and 1740 with $F_o^2 > 3\sigma(F_o^2)$. Atomic coordinates and isotropic thermal parameters are shown in Table 2. Complete anisotropic refinement on 124 variables resulted in a final $R/R_w$ = 3.8%/5.4%. Refinement of the enantiomorph did not yield a statistically better fit.

## Results and Discussion

**Structure.** The repeating unit of $Ba_6Ti_5S_{15}O$ is shown in Figure 1 and selected bond distances and angles are given in Table 3. The fragment features five Ti-centered, face-sharing octahedra, the actual asymmetric unit being half of this chain due to Ti(3) being positioned on a 2-fold axis. The Ti atoms are bonded exclusively to S atoms internally, but the chain's terminal faces are composed of bonds to two S atoms and one O atom. As mentioned, the parent compound, $BaTiS_3$, is composed of infinite chains of face-sharing [$TiS_6$] octahedra,[16] and so the formalism of the oxysulfide as $(BaO)(BaTiS_3)_5$ presents an accurate structural picture of the ternary compound being broken at every fifth octahedron by BaO.

The reconnection of the fragments in Figure 1 leads to a structure composed of two-dimensional anionic layers. A view perpendicular to these layers is given in Figure 2, and their corrugated nature is shown in the view parallel to the $a$ axis in Figure 3. The fragments are connected via corner sharing between the terminal octahedral. Only S(1) and O, both of which reside on 2-fold axes, are engaged in these linkages; the third atom, S(2), is terminal and directed into the interlayer gallery. The bridges formed by S(1) and O are nearly linear, and although linear bridges are commonly formed with oxygen, they are somewhat rare in the case of sulfur. Linear sulfide bridges have been

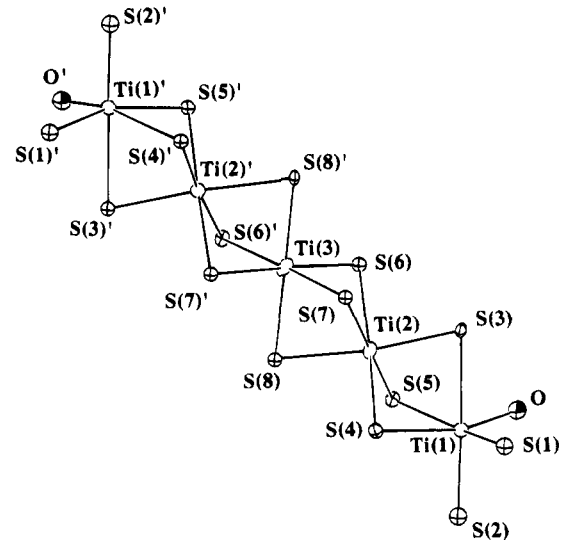


**Figure 1.** ORTEP drawing of the repeating unit of the anionic layers of $Ba_6Ti_5S_{15}O$, featuring five Ti-centered, face sharing octahedra. Ti atoms are represented by open ellipses; S atoms, by ellipses with no octant shading; O atoms, by ellipses with octant shading. Ti(3), S(1), and O all reside on 2-fold axes.

**Table 3. Selected Bond Distances (Å) and Angles (deg) for $Ba_6Ti_5S_{15}O$**

| | | | |
|---|---|---|---|
| Ti(1)−O | 1.868(4) | Ti(2)−S(3) | 2.382(4) |
| −S(1) | 2.444(3) | −S(4) | 2.286(5) |
| −S(2) | 2.252(4) | −S(5) | 2.242(5) |
| −S(3) | 2.671(4) | −S(6) | 2.604(5) |
| −S(4) | 2.690(5) | −S(7) | 2.384(5) |
| −S(5) | 2.433(5) | −S(8) | 2.465(4) |
| Ti(3)−S(6) | 2.362(5) | Ti(3)−S(8) | 2.414(3) |
| −S(7) | 2.506(5) | | |
| S(1)−Ti(1)−O | 101.3(1) | S(3)−Ti(2)−S(4) | 94.8(2) |
| −S(2) | 92.4(2) | −S(5) | 88.3(2) |
| −S(3) | 83.7(2) | −S(6) | 88.3(2) |
| −S(4) | 81.5(1) | −S(7) | 92.3(2) |
| −S(5) | 157.4(2) | −S(8) | 170.4(2) |
| S(2)−Ti(1)−O | 98.9(6) | S(4)−Ti(2)−S(5) | 94.9(2) |
| −S(3) | 174.3(2) | −S(6) | 174.0(2) |
| −S(4) | 95.5(2) | −S(7) | 100.4(2) |
| −S(5) | 99.0(2) | −S(8) | 94.7(2) |
| S(3)−Ti(1)−O | 86.0(6) | S(5)−Ti(2)−S(6) | 90.0(2) |
| −S(4) | 79.7(1) | −S(7) | 174.6(2) |
| −S(5) | 83.3(2) | −S(8) | 91.3(2) |
| S(6)−Ti(3)−S(6)′ | 97.4(3) | Ti(1)−O−Ti(1)[a] | 166(1) |
| −S(7) | 175.3(2) | Ti(1)−S(1)−Ti(1)[a] | 170.5(3) |
| −S(7)′ | 87.3(1) | Ti(1)−S(3)−Ti(2) | 76.4(1) |
| −S(8) | 88.5(2) | −S(4)− | 77.5(1) |
| −S(8)′ | 95.2(2) | −S(5)− | 79.0(1) |
| S(7)−Ti(3)−S(6)′ | 88.7(8) | Ti(2)−S(6)−Ti(3) | 75.2(1) |
| −S(7)′ | 88.1(2) | −S(7)− | 76.7(1) |
| −S(8) | 90.3(2) | −S(8)− | 76.9(1) |
| −S(8)′ | 85.6(2) | | |
| S(8)−Ti(3)−S(6)′ | 95.2(2) | | |
| −S(7)′ | 90.3(2) | | |
| −S(8)′ | 174.4(3) | | |

[a] Represents atom on the neighboring fragment.

(14) Walker, N., Stuart, D. *Acta Crystallogr.* **1983**, *A39*, 158−166.
(15) (a) Sheldrick, G. M. In *Crystallographic Computing 3*; Sheldrick, G. M., Kruger, C., Doddard, R., Eds.; Oxford University Press: Oxford, England, 1985; pp 175−189. (b) Gilmore G. J. *Appl. Crystallogr.* **1984**, *17* , 42−46.
(16) (a) Clearfield, A. *Acta Crystallogr.* **1963**, *16*, 134. (b) Huster, J. *Z. Naturforsch.* **1980**, *B35*, 775.

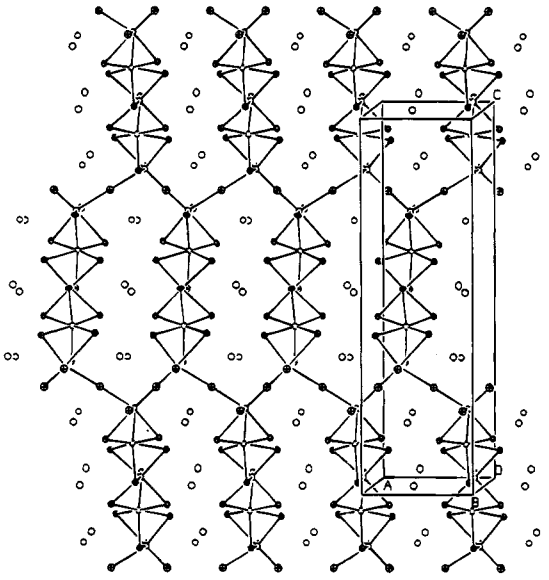

**Figure 2.** View down the $b$ axis of $Ba_6Ti_5S_{15}O$. The Ba atoms reside primarily in the cavities bounded by the chain fragments with slight protrusion into the interlayer gallery. Ti atoms are represented by small open ellipses; Ba atoms, by large open ellipses; S atoms, by ellipses with no octant shading; O atoms, by ellipses with octant shading.

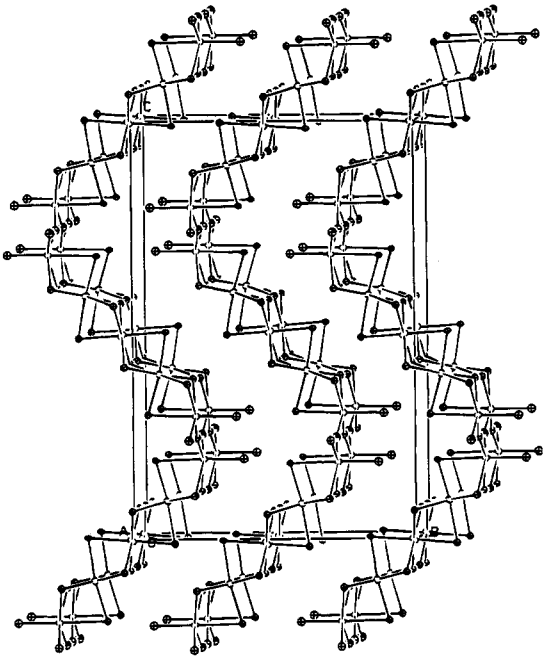

**Figure 3.** Anionic layers (Ba omitted) of $Ba_6Ti_5S_{15}O$ as viewed down the $a$ axis highlighting their corrugation.

seen in several Ba/Zr or Hf/S phases including $Ba_2ZrS_4$,[17a] $Ba_3Zr_2S_7$,[17a] $Ba_2HfS_4$,[17b] $Ba_6Hf_5S_{16}$,[17c] and $Ba_5Hf_4S_{13}$,[17c] all of which form perovskite-related structures. Interestingly, $BaMS_3$ (M = Zr, Hf) adopts the $GaFeO_3$ structure type, which is a perovskite derivative distorted by bent M–S–M bonds.[18] This leads us to speculate on the necessity of O for the formation of $Ba_6Ti_5S_{15}O$. Does the O force S(1) into a linear bridge or rather is an all-S analog, in fact, possible? We also note that while $BaTiS_3$ has face-sharing octahedra in which all Ti–S–Ti angles are bent, the compound $BaTiO_3$ has the perovskite structure-type, with all the $[TiO_6]$ units corner sharing through linear Ti–O–Ti angles. Hence, many different structure types may be accessible simply on the basis of varying the ratio of linear to bent M–X–M bridges.

An interesting feature of the anionic layers in $Ba_6Ti_5S_{15}O$ is the formation of intralayer cavities as seen in Figure 2. These cavities do not lead to channels through the layers as their position is staggered by half the length of the $a$-axis from layer to layer. However, they do form the primary location of the $Ba^{2+}$ atoms in the compound. From these cavities the $Ba^{2+}$ protrude only slightly into the interlayer gallery, leaving the spacing between the layers void. As such, $Ba_6Ti_5S_{15}O$ may exhibit intercalation chemistry, perhaps via a reduction of the $Ti^{4+}$ to $Ti^{3+}$ which could then be charge balanced by small cations such as $Li^+$ diffusing through the interlayer gallery. If favorable, such behavior could even make $Ba_6Ti_5S_{15}O$ a candidate for a rechargeable battery host material.

A small family of layered alkali/titanate compounds exists, which has some interesting structural similarities to $Ba_6Ti_5S_{15}O$. These compounds have the general formula $(A_2O)(TiO_2)_n$ where A = Na for $n$ = 3 ($Na_2Ti_3O_7$),[19] A = K for $n$ = 4 ($K_2Ti_4O_9$),[20] and A = Cs for $n$ = 5 ($Cs_2Ti_5O_{11}$).[21] Their structures are based on blocks of edge sharing $TiO_6$, $n$ octahedra long, which are fused together through further edge sharing into 1-D ribbons. The ribbons are then connected to each other through corners to form corrugated anionic layers, with the alkali ions filling the interlayer gallery. It has been shown that these compounds can be ion-exchanged to produce protonated forms which then have been studied extensively for their interesting intercalation chemistry.[22] Apparently the size of the $TiO_2$ fragments stabilized in this family is a function of the cation size as well as the $A_2O/TiO_2$ ratio. Larger cations stabilize larger fragments. As such perhaps $Ba_6Ti_5S_{15}O$ may already represent the optimum balance between cation size and chain fragment length. If this is so, future synthetic exploration of related phases could focus on the effect of changing cation sizes, both homoleptically and as a mixture of different alkaline-earth cations.

*Spectroscopic Data.* The optical absorption spectrum of $Ba_6Ti_5S_{15}O$ is shown in Figure 4. The onset of a sharp change in ($\alpha/S$) at approximately 1.04 eV corresponds to an estimate of the bandgap of this compound. Hence, $Ba_6Ti_5S_{15}O$ is expected to be a semiconductor. As in the semiconducting $TiS_2$ this absorption arises from the photon excitation of valence band electrons localized mainly on sulfur orbitals to the d-band orbital levels

(17) (a) Saeki, M.; Yajima, Y.; Onoda, M. *J. Solid State Chem.* **1991**, *92*, 286–294. (b) Chen, B.-H., Eichhorn, B. W. *Mater. Res. Bull.* **1991**, *26*, 1035–1037. (c) Chen, B.-H., Eichhorn, B. W., Fanwick, P. E. *Inorg. Chem.* **1992**, *31*, 1788–1791.

(18) Lelieveld, R.; Ijdo, D. J. W. *Acta Crystallogr.* **1980**, *B36*, 2223–2226.

(19) Andersson, S.; Wadsley, A. D. *Acta Crystallogr.* **1961**, *14*, 1245.

(20) (a) Verbaere, A.; Tournoux, M. *Bull Soc. Chim. Fr.* **1973**, 1237. (b) Dion, M., Piffard, Y.; Tournoux, M. *J. Inorg. Nucl. Chem.* **1978**, *40*, 917.

(21) (a) Grey, I. E.; Madsen, I. C.; Watts, J. A.; Bursill, L. A.; Kwiatkowska, J. *J. Solid State Chem.* **1985**, *58*, 350. (b) Kwiatkowska, J.; Grey, I. E.; Madsen, I. C.; Bursill, L. A. *Acta Crystallogr.* **1987**, *B43*, 258.

(22) (a) Marchand, R.; Brohan, L.; Tournoux, M. *Mater. Res. Bull.* **1980**, *15*, 1129. (b) Izawa, H.; Kikkawa, S.; Koizumi, M. *J. Phys. Chem.* **1982**, *86*, 5023. (c) Saski, T.; Watanabe, M.; Komatsu, Y.; Fujiki, Y. *Inorg. Chem.* **1985**, *24*, 2265. (d) Saski, T.; Watanabe, M.; Komatsu, Y.; Fujiki, Y. *Chem. Mater.* **1992**, *4*, 894–899.

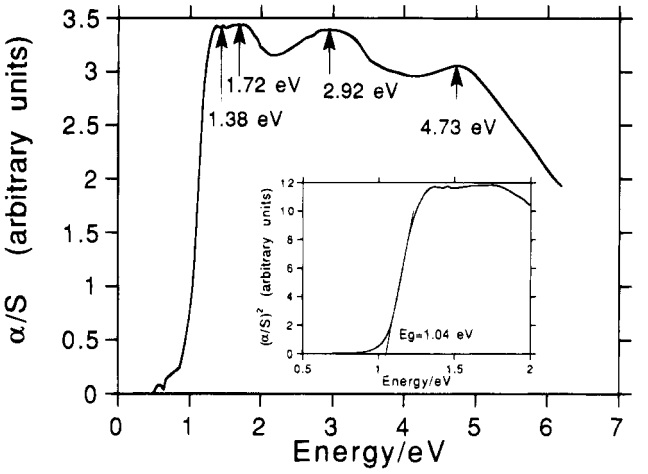


**Figure 4.** Plot of absorbance (arbitrary units) vs energy (eV) for $Ba_6Ti_5S_{15}O$. The inset graph shows absorbance squared vs energy. The onset of a sharp change in absorbance at 1.04 eV corresponds to an estimate of the material's band gap.

($t_{2g}$ type) of Ti. Also observed are several higher energy peaks at 1.38, 172, 2.92, and 4.73 eV.

The solid-state far-IR spectrum of $Ba_6Ti_5S_{15}O$ shows the following strong peaks: 418, 389, 359, 329, 292, 234, 209, 199, and 141 $cm^{-1}$. With the exception of the high energy 418 $cm^{-1}$ band, which is likely caused by Ti−O asymmetric vibrations, the variety of Ti−S bonds in the material make specific assignments of the peaks difficult.

## Conclusions

The new metal/oxysulfide $Ba_6Ti_5S_{15}O$ represents the first member in a potential new family of compounds with the general formula $(BaO)_n(BaTiS_3)_m$. Aside from being of potential interest as a layered intercalation host, the material represents a possible new direction in the underexplored area of solid-state oxychalcogenide chemistry. Specifically, it may be possible to use the high oxophilicity of early transition metal elements to drive structural modifications of known non-oxide starting materials by using only small amount of oxide to diffuse through and fragment the parent phase. Such chemistry would no doubt be facilitated by the use of starting phases of reduced dimensionality, as oxide ions could diffuse more readily through such materials. Although potentially accessible by stoichiometric combinations of starting materials, some manner of flux growth may be necessary to form single crystals suitable for structure determination and bulk physical measurements.

**Acknowledgment.** We wish to gratefully acknowledge the financial support of NSF and the NASA Graduate Student Researchers Program. Financial support from the National Science Foundation (DMR-92-02428) is also gratefully acknowledged. This work made use of the SEM facilities of the Center for Electron Optics at Michigan State University.

**Supplementary Material Available:** Listings of calculated and observed structure factors (12 pages). Ordering information is given on any current masthead page.